Using "Piecewise" to Solve Classes of Control Theory Problems

Martin von Mohrenschildt[‖]

Abstract: Differential equations with piecewise continuous coefficients or piecewise continuous perturbation often arise in physics and engineering. For example, forcing terms of electro-magnetic field type are often discontinuous in the presence of shielding materials. And in control theory, (optimal) controls are often discontinuous, for example, bang-bang optimality results. The author designed and implemented the new `piecewise` facility in Maple V Release 4. In this paper we show how to use symbolic methods using piecewise functions for control theory problems.

Introduction to Piecewise functions

In Maple V.4 the implementation of `piecewise` was replaced and the functionality significantly extended. The new implementation of piecewise is based on the theory of closed form solutions of ordinary differential equations with piecewise continuous coefficients [Moh94], [Moh95], [Moh96], [Jeffrey]. The theory provides a normal form for piecewise functions over the real axis, and an extension of the classical symbolic algorithms for integration and solutions of differential equations to equations whose coefficients are piecewise continuous functions. The symbolic approach to piecewise functions, in contrast to the numeric approach, allows us to manipulate piecewise functions where the boundary of the pieces can depend on parameters. Note, the default value if not provided as the last argument of piecewise is 0. For example

```
> assume(a>0);
> piecewise(x<0,-x,x);
```

$$\begin{cases} -x & x < 0 \\ x & \text{otherwise} \end{cases}$$

```
> convert(abs(a-"),piecewise,x);
```

$$\begin{cases} -x-a & x \le -a \\ a+x & x \le 0 \\ a-x & x \le a \\ x-a & a < x \end{cases}$$

Control theory

In mathematical control theory one tries to find an optimal control to a system modeled by a differential equation. The optimality of the control is determined by a side relation, often an integral, which is to be maximized or minimized. Given a differential equation

$$y' = f(y,u)$$

and a cost function $J(y(t),u(t))$ the problem of optimal control consists of finding the control function $u(t)$ such that the cost function J is maximized or minimized. We solve the problem by finding a *prototype control function* depending on parameters such that a certain instantiation of the parameters represents the optimal solution. This problem is in general unsolvable. But with appropriate constraints on the control function, for example, that it is bounded e.g., $-\alpha \le u(t) \le \beta$, classes of problems where the ansatz for the control functions is known can be identified. In these cases the Pontryagin maximum principle [Barnett75] predicts that the optimal bounded control function is piecewise continuous.

If we know the synthesis function u (the control function depending on parameters), then the problem of optimal striking, optimal control, can be solved using the theory underlying `piecewise`. This means, having an ansatz for the function $u(t)$, we have to solve a differential equation with piecewise perturbation or piecewise coefficients.

Example 1: parking a rocket car

We start with a simple illustrative example: The problem is to park a car. The car is initially stationary and has to be moved a certain distance d. This car is a so called rocket-car, since it uses fuel to brake.

The differential equation modeling the rocket-car with acceleration $u(t)$ is easily found:

$$y'' = u.$$

We study two different cost functions, one minimizes the parking time, the other takes fuel costs into consideration. The latter is realized by using a parameter k in the cost function J_2 indicating if it is more important to use less fuel, in which case k is small, or to park in less time. The smaller J_2, the less resources, time and fuel, we need to park.

$$J_1 = \int_0^T 1\,dt, \quad J_2 = \int_0^T k + |u|dt.$$

[‖]Electrical and Computer Engineering, McMaster University, Hamilton, Canada. email: mohrens@mcmaster.ca

The acceleration is bounded: $-1 \le u \le 1$ and we assume that the braking and acceleration forces are identical (rocket).

Time-optimal First we consider the problem of time-optimality by optimizing J_1. Given a fixed parking distance d, the goal is to park in minimum time T. Since the control function is bounded the control is bang-bang. It is clear from the modeled problem that there is one switch. $u(t)$ models maximum acceleration until time point $T/2$ and then maximum braking until T. We make the ansatz:

```
> u:=piecewise(t>=0 and t< T/2,1,t>=T/2
>     and t<T,-1);
```

$$u := \begin{cases} 1 & -t \le 0 \text{ and } t - 1/2\ \mathrm{T} < 0 \\ -1 & 1/2\ \mathrm{T} - t \le 0 \text{ and } t - \mathrm{T} < 0 \end{cases}$$

The formal parameter T (the total time) is positive. This leads to the following assumptions:

```
> assume(T>0);
```

```
> convert(u,piecewise,t);
```

$$u := \begin{cases} 0 & t \le 0 \\ 1 & t < 1/2\ \mathrm{T} \\ -1 & t < \mathrm{T} \\ 0 & \mathrm{T} \le t \end{cases}$$

Maple computes the solution of the model equation under the initial conditions $y(0) = 0$ and $D(y)(0) = 0$.

```
> dsolve({diff(y(t),t,t)=u,y(0)=0,D(y)(0)=0}
>     , y(t));
```

$$y(t) = \begin{cases} 0 & t \le 0 \\ 1/2\,t^2 & t \le 1/2\ \mathrm{T} \\ -1/2\,t^2 - 1/4\ \mathrm{T}^2 + t\,\mathrm{T} & t \le \mathrm{T} \\ 1/4\ \mathrm{T}^2 & \mathrm{T} < t \end{cases}$$

Note that the solution is constant for $t > T$, since the car stops at time point T. The parking distance is $\frac{T^2}{4}$. For a given distance d the shortest possible parking time is $2\sqrt{d}$. No further optimization is needed. Fig. 1 shows the position $y(t)$ of the car at time t with $T = 4$. The phase diagram Fig. 2 (x-axis: y(t), y-axis: y'(t)) shows two parabolic curves, the acceleration and braking.

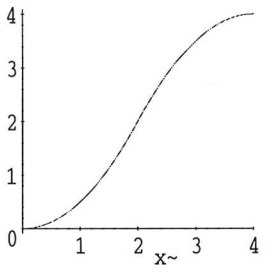

Rocket car, x-axis time t, y-axis path $y(t)$.

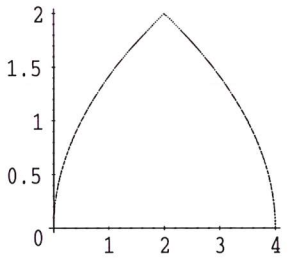

Phase diagram of car, x-axis $y(t)$ path, y-axis speed $y'(t)$.

Second, we examine the problem of **fuel cost**. The idea is to accelerate the car for a certain time b, let it coast, and then brake to a stop. The ansatz of the control function models maximum acceleration until time point b, coasting until time point $T - b$ where T is the total time, and then maximum braking until time T.

```
> u:=piecewise(t>=0 and t<b,1,t>T-b and
>     t<T,-1);
```

$$u := \begin{cases} 1 & -t \le 0 \text{ and } t - b < 0 \\ -1 & T - b - t < 0 \text{ and } t - T < 0 \end{cases}$$

The parameters must satisfy the following constraints; the time the car can accelerate has to be smaller than half the total time until we have to brake again, and the acceleration time is greater than 0. This results in the assumptions $b > 0, b < T/2$,

```
> assume(b>0,b<T/2);
```

```
> u:=convert(u,piecewise,t);
```

we get

$$u := \begin{cases} 0 & t \le 0 \\ 1 & t < b \\ 0 & t \le T - b \\ -1 & t \le T \\ 0 & T < t \end{cases}$$

Again we solve the differential equation assuming that the car is initially stationary.

```
> dsolve({diff(y(t),t,t)=u,y(0)=0,D(y)(0)=0},
>     y(t));
```

$$y(t) = \begin{cases} 0 & t \le 0 \\ t^2/2 & t \le \mathrm{b} \\ t\mathrm{b} - 1/2\,\mathrm{b}^2 & t \le \mathrm{T} - \mathrm{b} \\ -t^2/2 + \mathrm{T}\,\mathrm{b} + t\,\mathrm{T} - 1/2\,\mathrm{T}^2 - \mathrm{b}^2 & t \le \mathrm{T} \\ \mathrm{T}\,\mathrm{b} - \mathrm{b}^2 & \mathrm{T} < t \end{cases}$$

Again $y(t)$ is constant for $t > T$. The distance "driven" in time T is $y(T) = Tb - b^2$.

Next we compute the cost function

$$J_2 = \int_0^T k + |u| dt.$$

```
> J:=int(k+abs(u),t=0..T);
```

$$J := kT + 2b$$

Since the parking distance is $d = y(T) = Tb - b^2$ and the fuel efficiency factor is k, the optimal values for the parameters b and T of the control function can be computed using the above relation. For example if $d = 3$, and $k = 1/8$ then:

```
> solve(d=b*T-b*b,T);
```

$$\frac{d + b^2}{b}$$

```
> subs(T=",J):JJ:=subs(d=3,k=1/8,");
```

$$1/8\,\frac{3+b^2}{b}+2\,b$$

Now we compute the minimum of J:

```
> solve(diff(JJ,b)=0);evalf(");
```

$$1/17\sqrt{51}, -1/17\sqrt{51}$$

$$.4200840252, -.4200840252$$

If k decreases, meaning that fuel efficiency is more important, the acceleration time b decreases, and it takes longer to park the car. While, if k increases, we can park faster but need more fuel.

Plotting the phase diagram Fig. 3 we see the two parabolic curves joined with a straight line.

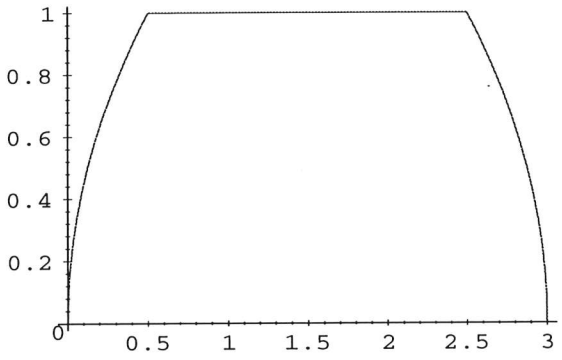

The phase diagram of fuel efficient parking. x-axis $y(t)$ path, y-axis speed $y'(t)$

Example 2: maximizing the fish harvest

We consider the stock of a species of fish. The aim is to maximize the total number of fish caught in a fixed amount of time. At the beginning of the fishing season the stock is filled up to maximum. The growth of the stock is assumed to be logistic. Fishing regulations set a maximum permitted rate for the harvesting of fish that is proportional to the size of the stock. The model equation (nonlinear) is

$$y' = 2y - y^2 - uy \quad 0 \le u \le k.$$

where y is the size of the stock and u is the harvesting rate, limited by k.

To get a "feeling" for the differential equation we plot solutions for different initial values (Figure 4): In [Guidera] this logistic differential equation is examined further.

```
> dsolve({diff(y(t),t)=2*y(t)-$y(t)^2$,
>        y(0)=a},y(t));
```

$$y(t) = 2\left(1 - \frac{e^{-2t}(-2+a)}{a}\right)^{-1}$$

```
> f:=unapply(rhs("),a):
> plot({f(1/2),f(1),f(5/4),f(2),f(5/2),f(3),
>       f(4)}, t=0..3);
```

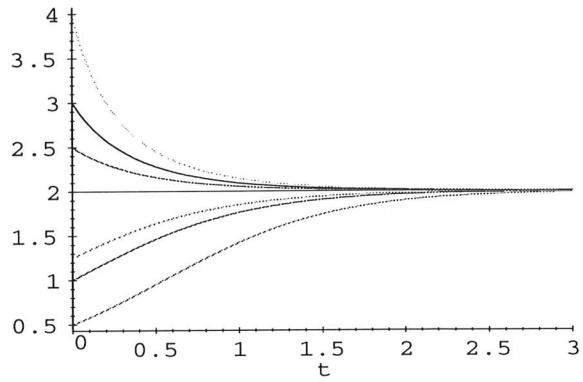

Solutions to the fish stock model equation with different initial conditions.

Note the nonlinearity of the model equation — the equation has an attractor at $y(t) = 2$. In this state as many fish are born as die.

The cost function J models the amount of fish harvested over the time T,

$$J = \int_0^T uy\, dt.$$

We make some assumptions: (i) the maximal fishing rate is bigger than the growth of the stock, (ii) the stock is maximal at the beginning and (iii) we have enough time T, longer than the time needed to fish the stock to zero. In our example we assume that the maximal permitted fishing rate is $\frac{5}{2}$. Following the Pontryagin maximum principle the control function is piecewise continuous. We make the ansatz for the control function. First, for the period a, we harvest with the maximum rate. Then we fish at the rate corresponding to the highest growth rate of the stock, which is the maximum of the right-hand side of our model equation,

```
> maximize(2*y-y*y);
```

$$1$$

resulting in 1. Near the end of the fishing season we will empty the stock with the maximal permitted rate.

```
> assume(0<a,a<b,T>b);

> u:=piecewise(t>0 and t<a,5/2,t>=a and
>          t<b,1,5/2):

> u:=convert(u,piecewise,t);
```

$$\begin{cases} 5/2 & t \le a \\ 1 & t < b \\ 5/2 & b \le t \end{cases}$$

```
> rhs(dsolve(diff(y(t),t)=2*y(t)-$y(t)^2$
>      -u*y(t),y(t)));
```

$$\begin{cases} -\dfrac{e^{\frac{3}{2}a-\frac{3}{2}b}}{2e^{\frac{3}{2}a-3/2b}-\frac{5}{2}e^{-\frac{3}{2}b+\frac{3}{2}a+\frac{1}{2}x}} & x \le a \\ -\dfrac{e^{\frac{3}{2}x-\frac{3}{2},b}}{3e^{-\frac{3}{2}b+a+\frac{1}{2}x}-e^{\frac{3}{2}x-\frac{3}{2}b}-5/2\,e^{\frac{-3}{2}b+\frac{3}{2}a+\frac{1}{2}x}} & x \le b \\ \dfrac{1}{-(3e^{-\frac{3}{2}b+a+\frac{1}{2}x}-3e^{\frac{1}{2}x-\frac{1}{2}b}+2-\frac{5}{2}e^{\frac{-3}{2}b+\frac{3}{2}a+\frac{1}{2}x}} & b < x \end{cases}$$

```
> sol:=":
```

Next we compute the integral $J = \int_0^T sol\ u\ dt$ which gives us the amount of fish caught over the period T. This calculation cannot be done with the help of numeric integration since we have to integrate the solution of a differential equation with parameters.

```
> J:=int(sol*  u,t=0..T);
```

$$\frac{5}{2}\ln(-4e^{\frac{3}{2}a}-\frac{3}{2b}+5e^{-\frac{3}{2}b+2a})+5b-6a+$$

$$+\ln(-6e^{a}+5e^{\frac{3}{2}a}+2e^{b})-\ln(-4+5e^{1/2a})+$$

$$\frac{5}{2}\ln(-6e^{a+1/2T}+5e^{\frac{3}{2}a+1/2T}+6e^{1/2T+b}-4e^{\frac{3}{2}b})$$

$$-\frac{5}{4}T-\frac{5}{2}\ln(-6e^{a+1/2b}+5e^{\frac{3}{2}a+1/2b}+2e^{\frac{3}{2}b})$$

The last step is to find the maximum of J for the parameters a and b. Plotting J gives a first feeling for the values for a and b. We compute the symbolic solution[1].

```
> res:=subs(T=10,J):diff(res,a):diff(res,b):

> solve({"","},{a,b}): evalf(");
```

$$\{b = 3.772588722, a = .3646431136\},$$

$$\{b = 5.964651630+6.283185308I, a = .0006796345112\},$$

$$\{b = 9.554380954, a = 9.554380954+6.283185308I\}$$

Assuming that T, the total time is limited by 10, we find that $a = .36$ and $b = 3.7$ is the optimal solution. Fig. 5 shows the stock size as we fish using the optimal control function. To verify, one can also compute a directly by computing the time the stock needs under the maximal fishing rate, u=$\frac{5}{2}$, to reduce the stock from 2 to 1.

```
> dsolve({diff(y(t),t)=2*y(t)-$y(t)^2$-
>     5/2*y,y(0)=2},y(t)):

> solve(rhs(")=1,t);
```

resulting in $a = 2\ \ln(6/5)$ with is 0.3646431136.

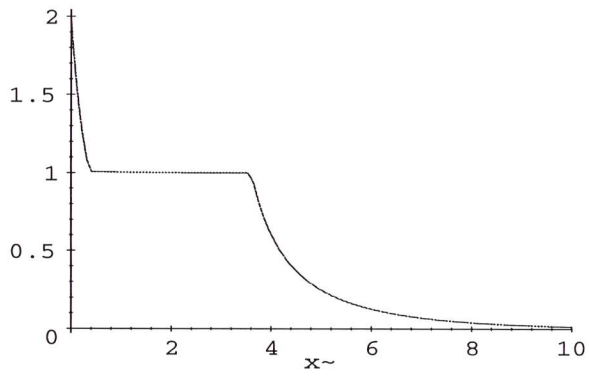

The size of the stock over one season.

Conclusion

We presented a method to solve certain control theory problems by using a symbolic ansatz for the control function, computing the symbolic solutions of the model equation which depend on parameters, and then optimizing the parameters to find the optimal control function. The main advantage of the approach can be seen in cases where the cost function depends on the solution of the model equation. In this case numerical methods are not suitable. The implementation of the new `piecewise` in MapleV.4 provides the functionality needed to handle symbolic solutions to these classes of problems.

References

[Barnett75] S. Barnett and R. Cameron: Introduction to mathematical control theory. *Oxford Applied Mathematics and Computations Series*, (1975).

[Moh94] M. von Mohrenschildt: Discontinuous ordinary differential equations. *PhD Thesis, Dept of Math., ETH Zurich, Nr. 10768*, (1994).

[1] This computation needs a large computer.

[Moh95] E. Engeler and M. von Mohrenschildt: The combinatory program. *Birkhäuser 1994*, (1995).

[Moh96] M. von Mohrenschildt: Normal forms for function fields containing piecewise functions *Technical Report Nr. 96-14 University of Waterloo*, (1997).

[Guidera] C. Guidera and M. Monagan: Teaching introductory differential equations with Maple *In same issue of MapleTech.*

[Jeffrey] D. Jeffrey, G. Labahn, M. v. Mohrenschildt: "Integration of signum and related functions", ISSAC'97.

Biography

Martin von Mohrenschildt received the Doctorate in mathematics from the ETH-Zurich in Switzerland in 1994. He spent two years 94–96 as a postdoctoral fellow at the Symbolic Computation Group of the University of Waterloo where he implemented, among other things, the new piecewise function, a pattern matcher, and a rule based programming system.

Since August 1996 he has worked as an Assistant Professor in the department of Electrical and Computer Engineering at McMaster University. He is appointed the junior chair in software engineering. His research interests include symbolic computation, formal software verification, and algebraic methods in software documentation.

Exploring the State Space Dimension of the Earth's Surface Mean Temperature: False Nearest Neighbors (FNN) Method

Rafael M. Gutierrez[†]

Abstract: The state space dimension of the earth's surface mean temperature is explored. The false nearest neighbors (FNN) method is used to investigate the embedding dimension of the temperature data. The surrogate data method gives some evidence to distinguish the temperature data from colored noise. The minimum dimension to unfold the possible attractor and the attractor dimension itself are estimated for a time scale of years.

Introduction

The atmosphere involves many processes with complex relations between them. The experimental data obtained from measurements of any observation of the atmosphere in general has important experimental limitations. Some of them are the limited precision of measurements, small data sets, different kinds of contamination such as noise, variety of experimental data acquisition methods for the same data set, different experimental errors, etc. These two aspects, the underlying complexity and the experimental limitations, can make atmospheric data appear "chaotic". In the old sense of the word, chaos implies a random or stochastic behavior. That is, an absolute absence of deterministic relations. Within the context of nonlinear dynamics the modern concept of chaos permits deterministic relations between the different degrees of freedom of a system.

Evolving methods in nonlinear dynamics are used to characterize and extract interesting and useful information from irregular signals. This information can be used in the construction of a deterministic model with a predictive power beyond statistical estimations. In this process, an important initial step is the estimation of the state space dimension of the system from a time series of measurements. The state space dimension is the minimum and sufficient number of variables needed to represent the system within a particular space and time scale.

The dimension of the state space can be estimated from the data with different methods. The most popular methods are: singular value decomposition [1, 2], saturation of system invariants [2, 3], the method of true vector fields [2], the box counting methods [1, 4, 5, 6], a new method of the power spectra [7], and the false nearest neighbors (FNN) method [2, 8, 9]. In this paper we implement the FNN method to show how it could give valuable information about the dynamics of the earth's surface mean temperature based on a small data set of experimental measurements.

It is important to point out the effects of having a small noisy data set. Noise is formally infinite dimensional, it always wishes to be unfolded in a larger dimension than the dynamical signal of interest requires. Therefore, the minimum dimension to unfold the dynamics may be shifted to larger dimensions and a small number of FNN may remain for any embedding dimension when the time series is contaminated with noise. An extensive study has shown that the FNN method is rather robust against contamination, in particular for normal noise [8]. The main reason for this is because the FNN method does not rest on distance evaluation for its accuracy as many other methods do [10]. This method is also fairly accurate for small amounts of data, as small as 100 observations [8]. However, for small and noisy data sets the sensitivity of a given system may be high and the results must be carefully judged understanding that the finest details of the attractor may be lost.

The data

The OAK Ridge National Laboratory provides synopsis of frequently used global-change data [11]. Of this valuable information, we will use the global temperature anomalies obtained from instrumental surface air temperature records compiled by K. Ya. Vinnikov, P. Ya. Groisman and K. M. Lugina. This data has been mainly taken from the *World Weather Records*, *Monthly Climatic Data for the World*, and *Meteorological Data for Individual Years over the Northern Hemisphere Excluding the USSR*. This information was completed and improved using other data and methods that are explained and referred to in reference [11].

The original set of data (1356 data points correspond to the 12 monthly mean temperatures from 1881 to 1993 in chronological order), is given with two decimal digits of accuracy. We transform this data in order to fully exploit the capability of Maple to perform exact rational arithmetic. With this we obtain improved precision and conciseness for repet-

[†]Physics Department, Group of Applied Science, New York University. On leave of absence from Centro Internacional de Fisica CIF, Santafé de Bogotá, COLOMBIA. Research supported in part by Colciencias, COLOMBIA, rmg4939@is.nyu.edu

itive operations on data of similar magnitude [12]. The data is initially stored in the list denoted by Tm.

We can transform the data into positive integers and subsequently transform the resulting floating point data into rational data preserving the chronological order. We store the rational data in the list Tmr.

```
> Tmr:=map(x->convert((x+1.2)*100,
> rational),Tm):
```

The sum of the 12 monthly data of each year divided by 12 gives the annual mean of the 113 years of data stored in the list Tan. Each of the N components of the list Tan is a positive rational within the range $61.0833, 171.5833$. In figure 1 we present the data stored in the list Tan where the years 1 to 113 correspond to 1881 to 1993.

```
> years:=[seq(i,i=1..N)]:
> pair:= (x,y) -> [x,y]:
> fig1:=zip(pair,years,Tan):
> plot(fig1,labels=[`year`,`anT`],
> tickmarks=[3,2]);
```

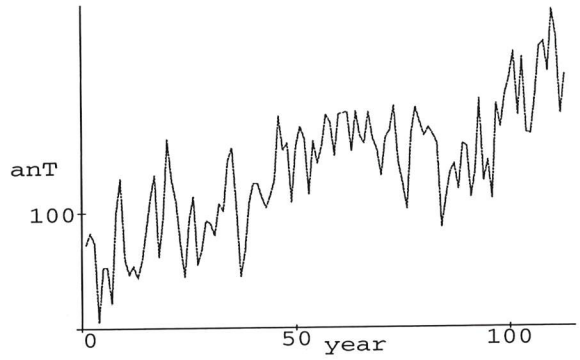

Figure 1: The data of the earth's surface mean temperature anomalies in positive rational numbers. The mean is taken annually, Tan, and the years 1 to 113 correspond to 1881 to 1993.

The False Nearest Neighbors (FNN) technique and its implementation

In order to have a real representation of the trajectories of any system in its state space, the dimension of a Euclidean space R^d must be large enough to unfold the dynamics of the system without ambiguity [2, 13]. This Euclidean space is called the embedding space and its dimension is the embedding dimension. The embedding dimension must show the closeness of two different points (states of the system at different times) when it really exists, not as a consequence of an artifact of having chosen d too small. If the chosen value is too large all of the system invariants can be uncovered, but this will result in greater computational costs [2]. Therefore, it is very important to estimate the minimum embedding dimension for a system with unknown state space dynamics. Topological arguments relate the dimension of the attractor in state space d_A, with the embedding dimension d, by $d_A \leq 2d + 1$ [2, 13, 14, 15]. The attractor is the subset of points of the state space to which the dynamics of the system is confined after trends have died out.

To reconstruct the embedding space from the time series of samples, we create a set of d-dimensional vectors. Our time series of measurements is represented by $x(n)$, where n indicates the time at which the measurement was made. The d-dimensional vectors are represented by $y(n) = [x(n), x(n+T), \cdots, x(n+(d-1)T]$. The components $x(n)$, $x(n+T)$, $\cdots, x(n+(d-1)T)$ are the delay coordinates of the vector or point $y(n)$ in the d-dimensional embedding space. The determination of the time delay T, requires information which is independent of the topological arguments. This allows any reasonable choice for T [2, 13, 14, 15].

In order to give a prescription of the optimal value of T some methods have been introduced [7, 9, 16, 17, 18, 19, 20, 21]. Some of these methods use a conditional probability of observing two different values at two different times. The most popular method of this kind uses the so-called average mutual information $I(t)$, defined by

$$I(t) = \sum P[x(n), x(n+t)] \times \log_2 \left(\frac{P[x(n), x(n+t)]}{P[x(n)]P[x(n+t)]} \right) \quad (1)$$

where the sum is taken over all the pairs $(x(n), x(n+t))$, and $P[x(n), x(n+t)]$ and $P[x(n)]$ are the conditional probability of observing the two data separated by time t, and the probability of independently observing the data $x(n)$ respectively. The first minimum of $I(t)$ is considered a good prescription for the time lag T [2, 9, 10]. However, as a prescription, values of T close to that of the first minimum must not change the results. Due to space limitations we do not show here the application of $I(t)$ to the temperature data. The $I(t)$ for the annual mean temperature data has a first broad weak minimum for values of t=1 or 2. When $I(t)$ does not show any clear minimum and it decreases fast it does not lose its role as a good selector of T. Without much grounds beyond intuition, T=1 or 2 are generally used, or choose T such that $I(t)/I(0) \sim 5$ [10]. We use T=1 which is consistent with these considerations.

The topological considerations of the FNN technique to estimate the state space dimension are based on the following methodology.

First, we embed the one dimensional time series $x(n)$ into d-dimensional vectors $y(n)$. For $d = 1$ we have $y(n) = x(n)$, for $d = 2$ we have $y(n) = [x(n), x(n+1)]$ and continuing to any dimension d we obtain $y(n) = [x(n), x(n+$

$1), \cdots, x(n + (d - 1))]$. For each of these different dimensional embeddings we find the nearest neighbor (NN) of each point $y(n)$.

The following procedure $MND(d)$ creates the $(N-(d-1)) \times d$ matrix $Tand$, for any dimension d. The rows are the d-dimensional points $y(n)$.

```
> MND:=proc(d::posint)
> local n, m;
> global N, Tand, Tan;
>   Tand:=matrix(N-d+1,d);
>   for n to N-d+1 do
>      for m to d do
>         Tand[n,m]:=Tan[n-1+m]
>   od od end:
```

The procedure $NND(d)$, finds the NN for each point $y(n)$ and the distances between each pair of points.

```
> NND := proc (d::posint)
>   local n,m,mid,midt,midtt;
>   global N,Tan, Rd1, near;
>  for n to N-d+1 do
>      mid:=10000. :
>      for m to N-d+1 do

> midt:=student[distance](row(Tand,n),
> row(Tand,m));

>        midtt:=evalf(midt);
>        if n<>m and midtt<mid then
>          mid:=midtt : near[n]:=m
>        fi od;
>      Rd1[n]:=mid
>    od end:
```

Second, we follow the method presented by Kennel, Brown and Abarbanel [8] to determine the false nearest neighbors FNN. This method consists of two criteria which must be satisfied simultaneously. The minimum value of d for which both criteria are satisfied is considered a good estimate of the embedding dimension.

The first criterion is given by

$$\frac{|x(n+d) - x^1(n+d)|}{R_d(n)} \geq Rtol \tag{2}$$

where $x(n+d)$ and $x^1(n+d)$ are the $d+1$ components of the d-dimensional point $y(n)$ and its respective NN. $R_d(n)$ is the distance between $y(n)$ and its NN in d-dimensions. $Rtol$ is some threshold value around 10 [8]. This criterion measures the ratio of the distance between a point and its d-dimensional NN in $(d+1)$-dimensions, to the distance between the same two points in d dimensions. With $Rtol = 10$, this inequality tells us that the distance between a point and its NN measured in $d+1$ dimensions is more than 10 times the distance between the same two points measured in d dimensions. When this happens, the NN is considered to become a false nearest neighbor (FNN).

The procedure $RTOLD(d, Rtol)$ finds the number of FNN using this first criterion.

```
> RTOLD := proc (d::posint,
> Rtol::positive)
> local n,FNN1;
> global Rd1, Tan, near,rtol, rtoll;
>   FNN1:=0;
>   for n to N-d-1 do
>     if Rd1[n]=0 then Rd1[n]:=1/1000 fi;
>      if near[n]< N-d and Rd1[n]<>500 then
>     rtol[n]:=abs(Tan[n+d+1]-
> Tan[near[n]+d+1])/Rd1[n]
>     else rtol[n]:=0 fi ;
>    if rtol[n]>Rtol then FNN1:=FNN1+1 fi;
>   od;
>  print(`FNN1=`, FNN1);
> end:
```

The implementation of the second criterion uses an estimate of the size of the attractor. The attractor is the Euclidean subspace spanned by the points $y(n)$. The size of the attractor Ra, is not very well defined. It can be estimated by either the size of the range of the data calculated above, the standard deviation of the data, or the estimation of Kennel et al.[8] given by

$$Ra^2 = \frac{1}{N}\sum_{n=1}^{N}[x(n) - \bar{x}]^2 \tag{3}$$

where

$$\bar{x} = \frac{1}{N}\sum_{n-1}^{N} x(n). \tag{4}$$

N is the number of data points ($N = 113$ annual means).

Since the attractor on any d-dimensional Euclidean space is finite, the distances between points and their NN cannot always increase as much as ten times or more. Therefore, the application of the first criterion to identify the FNN, will fail for those NN far from their corresponding points. That is, for values of $R_d(n) \approx Ra$. In these cases the second criterion gives an additional constraint. The FNN are identified when the distance of the point and its NN in $(d+1)$ dimensions becomes about twice the size of the attractor, $R_{d+1}(n) \approx 2Ra$[8]. For the second criterion the threshold parameter is $(R_{d+1}(n)/Ra) > Atol \approx 2$.

The procedure $RDRA(d, Atol, Ra)$ counts the number of FNN using the second criterion .

```
> RDRA := proc (d::posint,
> Atol::positive,Ra::positive)
>  local n,Rd1Ra,Rd1Raf, Tand1,FNN2;
>  global Tand;
>    FNN2:=0;
>   Tand1:=extend(Tand,0,1):
>    for n to N-d do
> Tand1[n,d+1]:=Tand1[n+1,1] od:
>   for n to N-d do
>      if near[n]<N-d then
>        Rd1Ra:=student[distance]
>  (row(Tand1,n),row(Tand1,near[n]))/Ra
>    fi;
>       Rd1Raf:=evalf(Rd1Ra):
>      if Rd1Raf > Atol then FNN2:=FNN2+1 fi
```

```
>     od;
>     print(`FNN2=`, FNN2);
> end:
```

The procedure $DIMENSION$, with parameters $Rtol$, $Atol$, Ra and $dmax$, incorporates all of the previous routines to find the number of FNN using the first and the second criteria. The procedure $NND()$ is included in $DIMENSION$ to replace the procedure $NND(d)$ for $d = 1$. The most time consuming instruction in $NND(d)$, which calculates the distances between points for any dimension, is replaced by a simple substraction of two values in $NND()$.

```
> DIMENSION :=proc(Rtol,Atol,Ra,dmax)
> local d;
> global N,Tan,Rd1,result;
> linalg[vector]
> (3*dmax);
>   for d to dmax do
>     print(`dimension=`,d); result[d]:=d;
>    MND(d);
>     if d=1 then
>       NND1() else
>       NND(d)  fi;
>     RTOLD(d,Rtol); result[d+1]:=FNN1;
>     RDRA(d,Atol,Ra); result[d+2]:=FNN2;
>   od end:
```

$DIMENSION$ can be used for different values of the two parameters $Rtol$ and $Atol$, the size of the attractor Ra, and for any dimension up to $dmax$. Nevertheless, since both criteria are parametrically independent, for certain calculations the use of only some of the routines in $DIMENSION$ can be more efficient than the whole procedure. It is particularly important when the use of the subprocedure $RDRA$ can be avoided.

Testing the method

In order to test the Maple code and the FNN method we have performed two different calculations. The first test analyzes data of a known dynamical system with and without noise added. This calculation tests the method and the code with small data sets and estimates the effects of noise. The second calculation applies the method of surrogate data which is used to differentiate chaotic determinism from colored noise [22].

For the first calculation we use 113 data points of one variable of the well known Lorenz model [23]. The Lorenz attractor has a fractal dimension (non-integer dimension) slightly larger than two (2.06), and the minimum dimension to unfold the Lorenz attractor is 3. The minimum embedding dimension is not necessarily the smallest integer larger than the attractor dimension. The Lorenz chaotic data is stored in the list $chalal$. We calculate the nominal size of the attractor as before to get $Ra \sim 8$. To add noise in different proportions to the chaotic data we write the following commands:

```
> readlib(rand): ranfe:=rand(-8..8):
> for n to 113 do
> chalan[n]:=chala[n]+ranfe()*p  od:
> chalanl:=convert(chalan,list):
```

The command $ranfe$ generates a random number within the nominal size of the attractor. This number is then multiplied by the parameter p which indicates the proportion of noise added to the clean chaotic signal. We then apply the same FNN procedures of section 3 to the chaos data with $p = 0, p = .05$ and $p = .2$ corresponding to clean or 0%, 5% and 20% noise added. In figure 2 we plot these results.

As expected, the clean data of the Lorenz model with embedding dimension 3 has zero FNN at $Rtol = 5$. When the data has noise the results change, i.e. the zero value of FNN for embedding dimension 3 is attained for larger values of $Rtol$, 9 and 13 for 5% and 20% of noise added respectively. It is also an expected result: The presence of noise tends to increase the dimension of the dynamics or, what may be equivalent, it tends to increase the value of $Rtol$ with which we obtain zero FNN at a fixed embedding dimension.

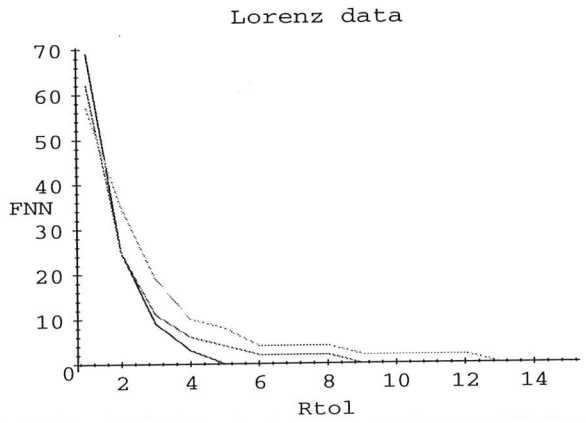

Figure 2: Lorenz chaotic data. The values of the tolerance parameter $Rtol$ at which the number of false nearest neighbors FNN, becomes zero for the fixed embedding dimension $d = 3$. For the clean data, 0% noise added, FNN=0 for $Rtol = 5$. For the same chaotic data with 5% and 20% of noise added we get FNN=0 for $Rtol = 9$ and $Rtol = 13$ respectively.

The second calculation gives some evidence to distinguish the temperature data from colored noise. The idea is to destroy the possible determinism underlying the time series maintaining linear aspects of the data set. The new data set is called the surrogate data. If a given characteristic of the dynamics has the same value for the original and the surrogate data, the low dimensional chaotic nature of the original data is doubtful. The unwindowed Fourier transform algorithm [22] generates a surrogate data consistent with a linear Gaussian process representing a colored random source. This surrogate procedure takes the Fourier transform of the data,

then the phase of each Fourier component is set to a random value, and finally the inverse Fourier transform is taken to go back to the time domain. This process preserves the correlation function and the power spectrum which are linear aspects of the data.

In order to implement the surrogate method using the fast Fourier transform available in MapleV4 (FFT), we increase the temperature data set from 113 to 128 data points by adding 15 data points equal to the mean value of the temperature time series ($\sim$ 110). The extended data is stored in the array $Taext$. This arbitrary extension of the original data generates small changes on the results of the FNN method. Our interest is to compare the extended data with expected determinism with its surrogate data without determinism. The extended original data is complemented with a list of 128 zeros, stored in the list $nadal$, for the corresponding imaginary parts and then the pairs are transformed using the FFT command. The randomization must be symmetric in order to obtain zero for all the imaginary parts of the data when the inverse Fast Fourier transform (iFFT) is applied. Next we present the Maple code to generate the surrogate data of the extended temperature time series.

```
> readlib(FFT):

> Taext:=array(1..128):
> nada:=array(1..128):

> for n to 113 do Taext[n]:=Tan[n]:
> nada[n]:=0 od:

> for n from 114 to 128 do
> Taext[n]:=110. :nada[n]:=0 od:

> FFT(7,Taext,nada):

> for n to 128 do
> faseT[n]:=arctan(nada[n]/Taext[n]) od:

> faseTl:=convert(faseT,list):

> ranfa:=rand(-1560958232..1560958231):
```

After FFT is applied, the conjugated phase of the first element is found for the element $N/2+1$, the second element corresponds to the last element N, the third corresponds to the element $N-1$, and so on, i.e. the conjugated pairs are $(1, N/2+1), (2, N), (3, N-1), \cdots, (N/2, N/2+2)$. The following commands randomize symmetrically the phases of the transformed time series

```
> alefas:=ranfa()/1000000000:
> faseT[1]:=alefas:faseT[65]:=-alefas:
> for n from 2 to 64 do
>   alefas:=ranfa()/1000000000. :
>    faseT[n]:=alefas :
>   faseT[128-n+2]:=-alefas :
>  od:
```

The array $faseT$ now has the symmetrically randomized phases. Next we calculate the real and complex part in polar form and then apply the iFFT.

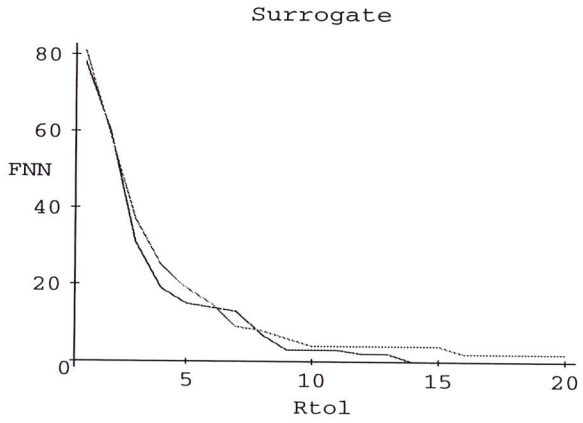

Figure 3: The extended data and its surrogate data from the temperature time series. For the extended data we get FNN=0 for $Rtol = 13$ with the embedding dimension fixed at $d = 3$. In the same conditions for the surrogate data the number of FNN never goes to zero.

In figure 3 we present the results of the FNN method applied to the original extended data and to the surrogate data for the fixed embedding dimension $d = 3$. For the surrogate data the number of FNN does not go to zero for $Rtol$ up to 20. For the extended data the FNN goes to zero for $Rtol = 14$. This result may indicate that the dynamics can be captured in a three-dimensional embedding space and that the determinism involved is lost when the data is surrogated. For different embedding dimensions the dynamics are not captured and so the surrogate data creates only minor changes, which actually happens for $d = 2$ and $d = 4$. Despite the small data set this may be evidence to distinguish the time series data from colored noise.

Results

The work of Kennel, Brown and Abarbanel [8] shows the robustness of the FNN method with respect to data with noise. It also gives the dependence on the values of the threshold parameters $Rtol$ and $Atol$, as well as the dependence on the size of the data set Ra. The conclusions were obtained from a careful and extensive application of the method to some well known chaotic systems, with and without added noise[8]. The time series of these systems were obtained from numerically solving the corresponding nonlinear equations or mappings.

In contrast, in this work we make a similar analysis for experimental data of the time series of the measured earth's surface mean temperature anomalies of the last 113 years. This implies naturally noisy data, a much smaller data set, and a highly complex and unknown state space dynamics of

the system. The corresponding differential equations or mappings are not known. Despite all of these limitations we find interesting results which can be useful for the construction of a model of this complex system.

For the first criterion we calculate the effects of the threshold $Rtol$. In figure 4, we have the number of FNN for $Rtol = 5$, 10 and 15, respectively.

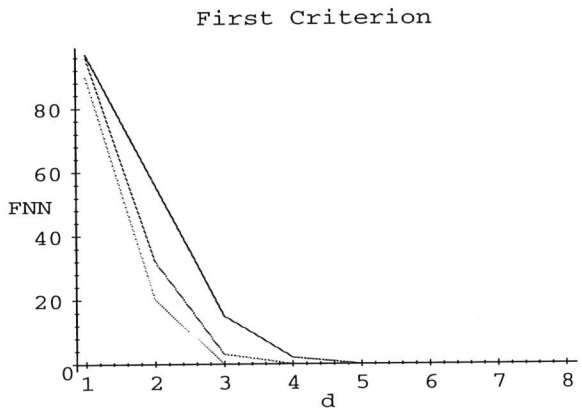

Figure 4: The number of FNN using the first criterion. The 3 lines correspond to $Rtol = 5, 10$ and 15 from the thinner to the thicker respectively.

As explained above, the value of d for which the number of FNN is zero gives an estimate of the embedding dimension. In figure 4, the results are $d = 3$, 4, and 5 for $Rtol = 5$, 10 and 15, respectively. Kennel et al. have shown that the effective embedding dimension degrades for a small data set ($N \sim 100$) and large $Rtol$. Topological arguments identify the FNN for $Rtol \geq 10$ however, this value may have to be adjusted considering the presence of noise and other particularities of the attractor and the time series representing it. From our results the value of $Rtol$ that best fits these two conditions is $Rtol = 10$. Therefore, the corresponding estimate of the embedding dimension is $d \simeq 4$.

For the second criterion with $Atol = 1.5$, 2, we calculate the number of FNN for $Ra = 21$, $Ra = 72$ and $Ra = 110$, figure 5,

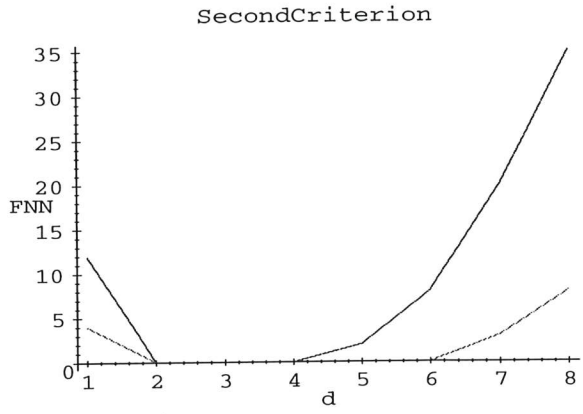

Figure 5: The number of FNN using the second criterion. The thinner line corresponds to $Atol = 1.5$ and the thicker one to $Atol = 2$. The attractor size is $Ra = 21$.

The number of FNN increases with increasing d after a small decrease. This behavior is less pronounced for $Atol = 1.5$ than for $Atol = 2$. If the size of the attractor $Ra = 21$ was a good estimate, these results could be evidence of a high-dimensional chaotic signal (noise), or a consequence of a high signal to noise ratio [8]. Both values of $Atol = 1.5, 2$, for $Ra = 72$ and $Ra = 110$ give zero FNN for any dimension d.

The first criterion estimates a low dimensional chaotic behavior of the earth's surface annual mean temperature, $d \sim 4$. The second criterion does not add conditions on the results of the first criterion for the number of FNN. If we consider the correct attractor size defined by Kennel et al. $Ra \sim 72$, the number of FNN given by the second criterion is always less than the number of FNN from the first criterion for any dimension d.

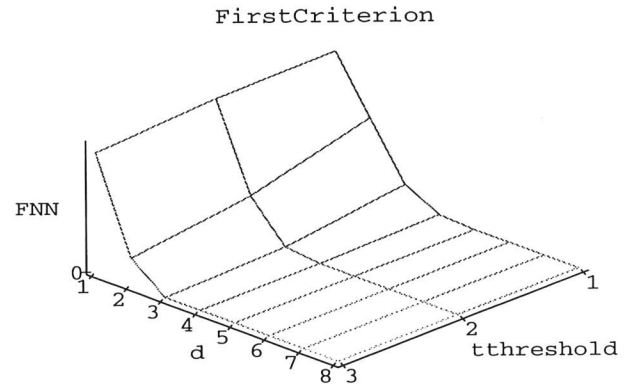

Figure 6: The number of FNN for the first criterion for $d = 1$ to 8. The three values in the first axis are $Rtol = 5$, 10 and 15 respectively.

Figures 6 and 7 show the domains of the threshold parameter $Rtol$ and the size of the attractor Ra, where it is valid to estimate the minimum embedding dimension. These domains are determined when the number of FNN is zero or very small, i.e. the flat regions of figures 6 and 7.

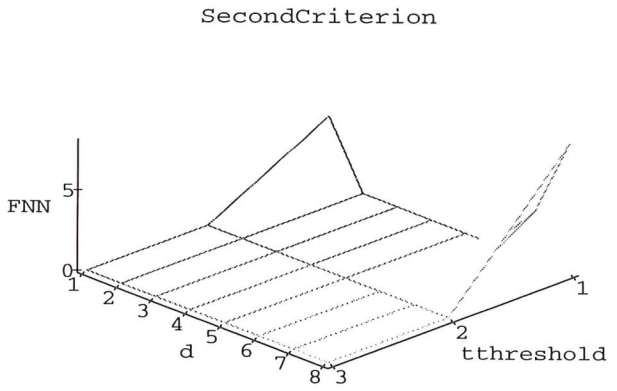

Figure 7: The number of FNN using the second criterion for $Atol = 2$ and $d = 1$ to 8. The three values in the first axis are the estimated size of the attractor $Ra = 21, 72$ and 110.

Conclusion

The FNN method estimates the minimum embedding dimension once the right range of the threshold parameters and the appropriate size of the attractor have been determined. Under these conditions the most suitable values of the different parameters are $Rtol \leq 10$, $Ra \leq 72$ and $Atol = 2$. The minimum embedding dimension will be the first dimension at which the number of FNN is zero for the two criterion. Figures 6 and 7 show that the two criterion are satisfied for an embedding dimension $d \sim 4$.

Using the surrogate data we have found evidence to differentiate the temperature data from colored noise however, some contamination is certainly present. The presence of noise in such a small data set may shift this estimate to larger dimensions, thus the actual minimum embedding dimension may be somehow smaller. Therefore, our estimate of the embedding dimension d cannot be more precise than $3 \leq d \leq 4$. In order to guarantee the preservation of all the dynamical and topological properties of the attractor in the embedding or reconstructed space, the attractor dimension d_A must be in the range $d_A \leq \frac{d-1}{2} \sim 1$ to $1.5 < 2$ [14, 15]. Although this range of dimensions for the attractor guarantees the conservation of all of its properties, the dimension of the attractor may be larger and all of its properties are still conserved for the same range of embedding dimensions.

In the context of nonlinear dynamics this result implies that the dynamics of the present complex system has only three or four active degrees of freedom. Thus, the earth's surface annual mean temperature represented by our time series could be modeled by a system of three or four coupled differential equations with some nonlinearities. These nonlinearities reduce the space where the solutions are confined, i.e. the attractor, to be less than two-dimensional. However, this conclusion is limited by the conditions of the data and the considerations we have made. Namely, the small data set, the unknown and untreated noise, the time delay prescription and the estimated value for the tolerance parameters.

References

[1] T. Mullin: *The nature of chaos.*, Oxford Univ. Press, New York, (1993).

[2] H. D. I. Abarbanel, R. Brown, J. Sidorowich and L. Sh. Tsimring: The analysis of observed chaotic data in physical systems, *Rev. Mod. Phys.*, **65**, pp. 1331–1392, (1993).

[3] M. Casdagli: Nonlinear prediction of chaotic time series, *Physica D*, **35**, p. 335, (1989).

[4] P. Grassberger and I. Procaccia: Characterization of strange attractors, *Phys. Rev. Lett.*, **50**, p. 346, (1983).

[5] J. D. Farmer and J. J. Sidorowick, in: *Evolution, learning, and cognition*, ed. Y. S. Lee, pp. 265–289, World Scientific, Singapore, (1988).

[6] A. A. Tsonis: *Chaos: From theory to applications.*, Plenum, New York, (1992).

[7] J. M. Lipton and K. P. Dabke: Reconstructing the state space of continuous time chaotic syatems using power spectra, *Phys. Lett. A*, **210**, (1996).

[8] M. B. Kennel, R. Brown and H. D. I. Abarbanel: Determining embedding dimension for phase-space reconstruction using a geometrical construction, *Phys. Rev. A*, **45**, pp. 3403–3411, (1992).

[9] W. Liebert and H. G. Schuster: Proper choice of the time delay for the analysis of chaotic time series, *Phys. Lett. A*, **142**, p. 107, (1989).

[10] H. D. I. Abarbanel: *Analysis of observed chaotic data* , Springer-Verlag, New York, (1996).

[11] T. A. Boden et al. eds.: *Trend'93, A Compendium of data on global change.*, Carbon Dioxide Information Analysis Center, Tennessee, (1994).

[12] K.M. Heal, M.L. Hansen and K.M. Rickard: *Maple V learning guide*, Waterloo Maple Inc., Waterloo, (1996).

[13] J.P. Eckman and D. Ruelle: Ergodic theory of chaos and strange attractors, *Rev. Mod. Phys.*, **57**, pp. 617–656, (1985).

[14] F. Takens: *Detecting strange attractors in turbulence, in dynamical systems and turbulence, Warwick 1980*, Lecture Notes in Mathematics, **898**, Springer, Berlin, pp. 366–381, (1980).

[15] R. Mané: *On the dimension of the compact invariant of certain nonlinear maps, in dynamical systems and turbulence, Warwick 1980*, Lecture Notes in Mathematics, **898**, Springer, Berlin, pp. 230–242, (1980).

[16] H.G. Schuster: *Deterministic chaos, an introduction*, VCH Verlagsgesellschaft, Weinhein, (1988).

[17] N. H. Packard, J. P. Crutchfield, J. D. Farmer, and R. S. Shaw: Geometry from a time series, *Phys. Rev. Lett.*, **45:9**, p. 712, (1980).

[18] D. S. Broomhead and G. P. King: Extracting qualitative dynamics from experimental data, *Physica D*, **20**, p. 217, (1985).

[19] D. Kugiumtzis: State space reconstruction parameters in the analysis of chaotic time series — the role of the time window length, *Physica D*, **95**, p. 13, (1996).

[20] M. T. Rosenstein, J. J. Collins, and C. J. De Luca: Reconstruction expansion as a geometry-based framework for choosing proper delay times, *Physica D*, **73**, p. 82, (1994).

[21] A. M. Fraser and H. L. Swinney: Independent coordinates for strange attractors from mutual information, *Phys. Rev. A*, **33**, pp. 1134–1140, (1986).

[22] J. Theiler, S. Eubank, A. Longtin, B. Galdrikian and J. D. Farmer: Testing for nonlinearity in time series: the method of surrogate data, *Physica D*, **58**, p. 77, (1992).

[23] E. N. Lorenz: Deterministic nonperiodic flow, *J. Atmos. Sc.*, **20**, p. 130, (1963).

Biography

Rafael M. Gutierrez obtained his degree in Physics from the Universidad Nacional de Colombia in Santafe de Bogota, Colombia, and his M.Sc. in solid state physics at the Universite de Montreal, Montreal-Canada. He has recently finished his Ph.D. at New York University, New York-USA in the Physics Department with the Applied Science group. His main interests are applications of new methods of nonlinear dynamics and chaos theory to construct phenomenological models in areas as diverse as solid state physics, particle physics and geophysics. Email: rmg4939@is.nyu.edu

Use of Maple V to Solve a Multi-Variable Optimal Control Problem in Fertilizer Economics

*Simon Woodward**

Abstract: Optimal control problems involve calculating the optimal inputs to a dynamical system over time in order to maximize some objective function. The example described here is the optimal application of phosphorus and sulphur fertilizer to grazed pastures on New Zealand livestock farms, in order to maximize the net present value of farm profits for ten years into the future. Maple is used to solve the Maximum Principle and Adjoint equations, and to generate computer code to calculate almost-optimal fertilizer policies. This code was used in a software package, Outlook™, which is designed to assist farmers in planning their fertilizer expenditure.

Introduction

Optimal fertilizer application involves trading off between the costs of buying and spreading fertilizer and the benefits of increased farm production. This is complicated because fertilizer nutrients carry over in the soil from one year to the next, so that investment in fertilizer in the present contributes a stream of benefit through future years.

We have developed proprietary decision support software, named Outlook™, to assist New Zealand sheep, beef, and dairy farmers in planning their fertilizer expenditure on a 10-year time horizon. Outlook™ models the changes in soil nutrient status from year to year resulting from application of fertilizer, predicts the resulting pasture and animal production, and calculates the profit. This enables a farmer or farm consultant to assess the relative profitability of different fertilizer policies.

As well as simulating given policies, Outlook™ is able to calculate the long term profit-maximising fertilizer policy. This is done by applying optimal control theory to the nutrient dynamics equations. The original version of Outlook™ considered only phosphate dynamics [2] and the economic optimization of that model is described in Woodward [5]. The software has now been updated to consider the coupled dynamics of both phosphorus and sulphur, the two most important nutrients in New Zealand pastoral farming. This paper describes how Maple V was used to generate the economic optimization subroutine in this latest version of Outlook™.

Nutrient dynamics

The biological basis for the software is a dynamic nutrient carryover model, described in Metherell *et al.* [3]. This is a coupled system of four difference equations describing the carryover of soil phosphate (P), unoxidized elemental sulphur ($E0$), above-equilibrium soil sulphate (S), and phosphate-extractable organic soil sulphur (Q).

*AgResearch Whatawhata, Hamilton, New Zealand.
woodwards@agresearch.cri.nz

Some of these terms require additional explanation. Firstly, P is a conceptual measure of total plant available phosphorus, including both organic and inorganic components. It is calibrated to Olsen extractable phosphorus [2]. Secondly, although the phosphate extraction technique extracts only a fraction of soil organic sulphur, phosphate extractable sulphur (Q) is used as a representative for total organic sulphur, since Q is well correlated to pasture yield. Thirdly, immediately following fertilizer application soil sulphate levels rise sharply and increases in pasture yield are observed. These transient effects are represented by the variable S. Thereafter sulphate levels rapidly drop to a low level in equilibrium with organic sulphur, at which time S tends to zero and the effect of sulphate on pasture growth is subsumed into the effect of Q.

Initial soil nutrient status ($P(1)$, $E0(1)$, $S(1)$, $Q(1)$) is determined from soil testing and fertilizer history. The dynamics equations take the form (using P as an example),

$$P_{t+1} - P_t = \mathrm{f}\,(P_t, E0_t, S_t, Q_t, FP_t, FE0_t, FS_t)$$

where FP_t, $FE0_t$ and FS_t are respectively the rates of P, $E0$, and S fertilizer application at the start of year t. We denote the right hand side EP.

Soil phosphate (P) cycling is affected by four main processes. Firstly there are contributions of phosphate from fertilizer, FP. Secondly, there is slow release of phosphate in the soil, Ps. Thirdly, there are losses of P and FP to various processes in the soil, $\beta(P + FP)$. And lastly, there is a term for the loss of P due to uptake and transfer by grazing animals. The change in P status from year to year is then:

```
> EP:=-beta*(P+FP)+Ps+FP-(a1*RHp+a2)*RY;
```

$$EP := -\beta\,(P + FP) + Ps + FP - (a1\ RHp + a2)\ RY$$

RHp is the relative concentration of phosphorus in the herbage, and depends upon the P fertility:

```
> RHp:=1-exp(-hP*soilP);
```

$$RHp := 1 - \mathrm{e}^{(-hP\ soilP)}$$

MapleTech Vol. 4, No. 3, pp. 46–51; ISSN 1061-5733